molecules

MDPI

Article

Metabolites of Siamenoside I and Their Distributions in Rats

Xue-Rong Yang [1], Feng Xu [2,*], Dian-Peng Li [1,*], Feng-Lai Lu [1], Guang-Xue Liu [2], Lei Wang [1], Ming-Ying Shang [2], Yong-Lin Huang [1] and Shao-Qing Cai [2]

1 Guangxi Key Laboratory of Functional Phytochemicals Research and Utilization, Guangxi Institute of Botany, Guangxi Zhuang Autonomous Region and Chinese Academy of Sciences, No. 85, Yanshan Road, Yanshan District, Guilin 541006, China; yxrxl@sina.cn (X.-R.Y.); lufenglai@126.com (F.-L.L.); ww8304@126.com (L.W.); hyl@gxib.cn (Y.-L.H.)

2 State Key Laboratory of Natural and Biomimetic Drugs, School of Pharmaceutical Sciences, Peking University, No. 38 Xueyuan Road, Beijing 100191, China; guangxl@bjmu.edu.cn (G.-X.L.); myshang@bjmu.edu.cn (M.-Y.S.); sqcai@bjmu.edu.cn (S.-Q.C.)

* Correspondence: xufeng_pharm@163.com (F.X.); ldp@gxib.cn (D.-P.L.); Tel.: +86-10-8280-2534 (F.X.); +86-773-355-0682 (D.-P.L.); Fax: +86-10-8280-2534 (F.X.); +86-773-355-0067 (D.-P.L.)

Academic Editor: Derek J. McPhee
Received: 3 January 2016; Accepted: 27 January 2016; Published: 30 January 2016

Abstract: Siamenoside I is the sweetest mogroside that has several kinds of bioactivities, and it is also a constituent of Siraitiae Fructus, a fruit and herb in China. Hitherto the metabolism of siamenoside I in human or animals remains unclear. To reveal its metabolic pathways, a high-performance liquid chromatography-electrospray ionization-ion trap-time of flight-multistage mass spectrometry (HPLC-ESI-IT-TOF-MS^n) method was used to profile and identify its metabolites in rats. Altogether, 86 new metabolites were identified or tentatively identified, and 23 of them were also new metabolites of mogrosides. In rats, siamenoside I was found to undergo deglycosylation, hydroxylation, dehydrogenation, deoxygenation, isomerization, and glycosylation reactions. Among them, deoxygenation, pentahydroxylation, and didehydrogenation were novel metabolic reactions of mogrosides. The distributions of siamenoside I and its 86 metabolites in rat organs were firstly reported, and they were mainly distributed to intestine, stomach, kidney, and brain. The most widely distributed metabolite was mogroside IIIE. In addition, eight metabolites were bioactive according to literature. These findings would help to understand the metabolism and effective forms of siamenoside I and other mogrosides *in vivo*.

Keywords: *Siraitia grosvenorii*; mogrosides; siamenoside I; metabolism; distribution; LC-IT-TOF-MS^n; natural sweeteners; saponins; cucurbitanes

1. Introduction

Mogrosides are a group of cucurbitane-type triterpenoid saponins which have the common aglycone of mogrol [1]. They are responsible for the sweet taste and bioactivities of Siraitiae Fructus (Luo Han Guo in Chinese, the ripe fruits of *Siraitia grosvenorii*), a traditional Chinese medicine and an edible fruit [2].

Siamenoside I is one of the mogrosides, which is firstly isolated from *Siraitia siamensis* (a Chinese folk medicine) [3] and then from *Siraitia grosvenorii* [4]. Its relative sweetness (0.01% solution) to 5% sucrose is determined to be 563, higher than the famous sweetener mogroside V, making it the sweetest cucurbitane glycoside [4].

Besides its intense sweet taste, siamenoside I also has several kinds of bioactivities. It can inhibit the induction of Epstein–Barr virus early antigen (EBV-EA) by 12-*O*-tetradecanoylphorbol-13-acetate

(TPA) in Raji cells, which implies that it is a potential cancer chemopreventive agent [5]. It also inhibits two-stage carcinogenesis induced by 9,10-dimethyl-1,2-benzanthracene (DMBA) and TPA in mice [6]. Furthermore, it exhibits a maltase inhibitory effect with IC_{50} value of 10 mM, which is more potent than those of mogroside V and mogroside IV (IC_{50} of 14 mM and 12 mM, respectively) [7].

In order to clarify the action mechanisms of the beneficial effects of mogrosides and to develop them into new health foods or drugs or sweeteners, it is necessary to investigate their metabolism and disposition. Up to now, there are only three reports on the metabolism of mogrosides. The first is about the human intestinal microflora biotransformation of mogroside III [8]; the second is on the *in vivo* digestion, absorption and metabolism of 72% mogroside V in rats [9], and the third is our study on the *in vitro*, *in vivo* metabolism of mogroside V (purity >98%) and the distributions of its metabolites in rats [10]. We find that mogroside V can be metabolized to its secondary glycosides and the aglycone morgol, and then morgol is oxidized to lots of metabolites. However, there are no reports on the metabolism of siamenoside I so far.

Although the importance of studying drug distribution in various organs is well established in the drug development field, the studies on the distributions of metabolites of bioactive natural products are neglected. Since our previous research indicates that the metabolites of natural products distribute unevenly in different organs of rats, such as mogroside V [10] and (+)-catechin [11], we believe that revealing the distributions of a bioactive natural product and its metabolites can be helpful in understanding its target organ and organ-specific bioactivities.

Accordingly, in the present work, the metabolites of siamenoside I and the distributions of siamenoside I and its metabolites in rats were firstly investigated by high-performance liquid chromatography-electrospray ionization-ion trap-time of flight-multistage mass spectrometry (HPLC-ESI-IT-TOF-MS^n). In total, 86 new metabolites of siamenoside I in rats were detected and identified or tentatively identified, and the metabolic pathways and *in vivo* processes of siamenoside I were proposed. Siamenoside I and its metabolites were mainly distributed to intestine, stomach, kidney, and brain, and mogroside IIIE was the most widely distributed metabolite.

2. Results

2.1. Profiling the Metabolites of Siamenoside I in Different Biosamples by HPLC-ESI-IT-TOF-MS^n

Based on the strategy described in Section 4.7, 86 new metabolites (**M1–M86**) of siamenoside I were detected altogether in different drug-containing samples by the HPLC-ESI-IT-TOF-MS^n technique (Table 1, Table S1, Figure 1, and Figures S1–S25).

Eighty-three metabolites were detected in drug-containing feces; 19 metabolites were found in urine, and only two were detected in plasma.

As for different organs, 2, 7, 7, 3, 13, 21, 19, and 14 metabolites were detected in heart, liver, spleen, lungs, kidneys, stomach, intestine, and brain, respectively. Furthermore, no metabolites were detected in muscles.

2.2. Identification of the Metabolites of Siamenoside I in Different Biosamples by HPLC-ESI-IT-TOF-MS^n

Nine new metabolites of siamenoside I were unambiguously identified to be mogroside IVA (**M3**), mogroside IVE (**M4**), mogroside III (**M8**), mogroside IIIE (**M9**), mogroside $IIIA_1$ (**M10**), mogroside IIE (**M15**), mogroside IIA_2 (**M17**), 11-oxomogroside IIE (**M20**), and mogrol (**M29**) sequentially by comparison of their LC-MS^n data to those of reference compounds.

The other 77 metabolites were tentatively identified by interpretation of their LC-MS^n data and by comparison with literature.

These 86 new metabolites of siamenoside I can be classified into 24 classes according to their formative reactions and molecular formulae.

Table 1. LC-MS data of siamenoside I and its 86 metabolites formed in rats and their formative reactions.

No.	t_R (min)	Meas. (Da)	Pred.(Da)	Err. (ppm)	DBE [2]	Formula	Identification	Reactions
M0 [1]	24.966	1169.5959	1169.5961	0.17	9	$C_{54}H_{92}O_{24}$	siamenoside I	−
M1	25.698	1285.6444	1285.6434	0.78	10	$C_{60}H_{102}O_{29}$	mogroside V isomer	+Glc
M2	26.043	1285.6441	1285.6434	0.54	10	$C_{60}H_{102}O_{29}$	mogroside V isomer	+Glc
M3 [1]	25.345	1169.5905	1169.5961	−0.09	9	$C_{54}H_{92}O_{24}$	mogroside IVA	isomerization
M4 [1]	25.960	1169.5923	1169.5961	−3.25	9	$C_{54}H_{92}O_{24}$	mogroside IVE	isomerization
M5	26.696	1169.5950	1169.5961	−0.94	9	$C_{54}H_{92}O_{24}$	mogroside IV isomer	isomerization
M6	25.923	1167.5730	1167.5804	−2.23	10	$C_{54}H_{90}O_{24}$	dehydrogenated siamenoside I	−2H
M7	25.983	1153.5957	1153.6011	−4.25	9	$C_{54}H_{92}O_{23}$	deoxygenated siamenoside I	−O
M8 [1]	26.803	1007.5425	1007.5432	−0.69	8	$C_{48}H_{82}O_{19}$	mogroside III	−Glc
M9 [1]	27.173	1007.5387	1007.5432	−4.47	8	$C_{48}H_{82}O_{19}$	mogroside IIIE	−Glc
M10 [1]	30.217	1007.5376	1007.5432	−5.56	8	$C_{48}H_{82}O_{19}$	mogroside $IIIA_1$	−Glc
M11	30.525	1007.5395	1007.5432	−3.67	8	$C_{48}H_{82}O_{19}$	mogroside III isomer	−Glc
M12	30.940	1007.5385	1007.5432	−4.66	8	$C_{48}H_{82}O_{19}$	mogroside III isomer	−Glc
M13	26.927	1005.5269	1005.5276	0.70	9	$C_{48}H_{80}O_{19}$	dehydrogenated mogroside III isomer	−Glc − 2H
M14	27.728	991.5441	991.5483	−4.24	8	$C_{48}H_{82}O_{18}$	deoxygenated mogroside III isomer	−Glc − O
M15 [1]	29.365	845.4881	845.4904	−2.72	7	$C_{42}H_{72}O_{14}$	mogroside IIE	−2Glc
M16	30.648	845.4944	845.4904	4.73	7	$C_{42}H_{72}O_{14}$	mogroside II isomer	−2Glc
M17 [1]	31.775	845.4910	845.4904	0.71	7	$C_{42}H_{72}O_{14}$	mogroside IIA_2	−2Glc
M18	33.298	845.4884	845.4904	−2.37	7	$C_{42}H_{72}O_{14}$	mogroside II isomer	−2Glc
M19	33.905	845.4918	845.4904	1.66	7	$C_{42}H_{72}O_{14}$	mogroside II isomer	−2Glc
M20 [1]	29.908	843.4737	843.4748	−1.30	8	$C_{42}H_{70}O_{14}$	11-oxomogroside IIE	−2Glc − 2H
M21	33.604	843.4726	843.4748	−2.61	8	$C_{42}H_{70}O_{14}$	dehydrogenated mogroside II isomer	−2Glc − 2H
M22	34.028	829.4946	829.4955	−1.08	7	$C_{42}H_{72}O_{13}$	deoxygenated mogroside II isomer	−2Glc − O
M23	34.813	827.4780	827.4798	−2.18	8	$C_{42}H_{70}O_{13}$	dehydrogenated deoxygenated mogroside II isomer	−2Glc − 2H − O
M24	34.997	683.4348	683.4376	−1.76	6	$C_{36}H_{62}O_9$	mogroside IA_1	−3Glc
M25	37.507	683.4366	683.4376	1.46	6	$C_{36}H_{62}O_9$	mogroside IE_1	−3Glc
M26	36.120	681.4196	681.4219	−3.38	7	$C_{36}H_{60}O_9$	dehydrogenated mogroside I isomer	−3Glc − 2H
M27	38.860	681.4215	681.4219	−0.59	7	$C_{36}H_{60}O_9$	dehydrogenated mogroside I isomer	−3Glc − 2H
M28	45.978	521.3834	521.3848	−2.69	5	$C_{30}H_{52}O_4$	mogrol isomer	−4Glc
M29 [1]	46.467	521.3838	521.3848	−1.92	5	$C_{30}H_{52}O_4$	mogrol	−4Glc
M30	52.478	519.3676	519.3691	−2.89	6	$C_{30}H_{50}O_4$	dehydrogenated mogrol	−4Glc − 2H
M31	52.953	519.3687	519.3691	−0.77	6	$C_{30}H_{50}O_4$	dehydrogenated mogrol	−4Glc − 2H
M32	23.007	553.3721	553.3746	−4.52	5	$C_{30}H_{52}O_6$	dihydroxylated mogrol	−4Glc + 2O
M33	26.528	553.3699	553.3746	−8.49	5	$C_{30}H_{52}O_6$	dihydroxylated mogrol	−4Glc + 2O
M34	27.482	553.3717	553.3746	−5.24	5	$C_{30}H_{52}O_6$	dihydroxylated mogrol	−4Glc + 2O
M35	28.152	553.3740	553.3746	−1.08	5	$C_{30}H_{52}O_6$	dihydroxylated mogrol	−4Glc + 2O
M36	26.475	551.3559	551.3589	−5.40	6	$C_{30}H_{50}O_6$	dehydrogenated dihydroxylated mogrol	−4Glc − 2H + 2O

Table 1. *Cont.*

No.	t_R (min)	Meas. (Da)	Pred.(Da)	Err. (ppm)	DBE [2]	Formula	Identification	Reactions
M37	27.050	551.3557	551.3589	−5.80	6	$C_{30}H_{50}O_6$	dehydrogenated dihydroxylated mogrol	−4Glc − 2H + 2O
M38	29.487	551.3566	551.3589	−4.17	6	$C_{30}H_{50}O_6$	dehydrogenated dihydroxylated mogrol	−4Glc − 2H + 2O
M39	30.887	551.3558	551.3589	−5.62	6	$C_{30}H_{50}O_6$	dehydrogenated dihydroxylated mogrol	−4Glc − 2H + 2O
M40	31.537	551.3561	551.3589	−5.04	6	$C_{30}H_{50}O_6$	dehydrogenated dihydroxylated mogrol	−4Glc − 2H + 2O
M41	33.122	551.3549	551.3589	−7.25	6	$C_{30}H_{50}O_6$	dehydrogenated dihydroxylated mogrol	−4Glc − 2H + 2O
M42	16.305	569.3655	569.3695	−7.03	5	$C_{30}H_{52}O_7$	trihydroxylated mogrol	−4Glc + 3O
M43	16.728	569.3671	569.3695	−4.22	5	$C_{30}H_{52}O_7$	trihydroxylated mogrol	−4Glc + 3O
M44	17.280	569.3660	569.3695	−6.15	5	$C_{30}H_{52}O_7$	trihydroxylated mogrol	−4Glc + 3O
M45	18.140	569.3674	569.3695	−3.69	5	$C_{30}H_{52}O_7$	trihydroxylated mogrol	−4Glc + 3O
M46	18.923	569.3675	569.3695	−3.51	5	$C_{30}H_{52}O_7$	trihydroxylated mogrol	−4Glc + 3O
M47	21.464	569.3675	569.3695	−3.51	5	$C_{30}H_{52}O_7$	trihydroxylated mogrol	−4Glc + 3O
M48	21.755	569.3674	569.3695	−3.69	5	$C_{30}H_{52}O_7$	trihydroxylated mogrol	−4Glc + 3O
M49	22.121	569.3666	569.3695	−5.09	5	$C_{30}H_{52}O_7$	trihydroxylated mogrol	−4Glc + 3O
M50	22.531	569.3667	569.3695	−7.03	5	$C_{30}H_{52}O_7$	trihydroxylated mogrol	−4Glc + 3O
M51	11.410	567.3489	567.3539	−8.80	6	$C_{30}H_{50}O_7$	dehydrogenated trihydroxylated mogrol	−4Glc − 2H + 3O
M52	18.482	567.3463	567.3539	−13.4	6	$C_{30}H_{50}O_7$	dehydrogenated trihydroxylated mogrol	−4Glc − 2H + 3O
M53	19.893	567.3534	567.3539	−2.64	6	$C_{30}H_{50}O_7$	dehydrogenated trihydroxylated mogrol	−4Glc − 2H + 3O
M54	20.977	567.3494	567.3539	−0.88	6	$C_{30}H_{50}O_7$	dehydrogenated trihydroxylated mogrol	−4Glc − 2H + 3O
M55	21.761	567.3512	567.3539	−7.93	6	$C_{30}H_{50}O_7$	dehydrogenated trihydroxylated mogrol	−4Glc − 2H + 3O
M56	22.365	567.3507	567.3539	−4.76	6	$C_{30}H_{50}O_7$	dehydrogenated trihydroxylated mogrol	−4Glc − 2H + 3O
M57	24.123	567.3497	567.3539	−5.64	6	$C_{30}H_{50}O_7$	dehydrogenated trihydroxylated mogrol	−4Glc − 2H + 3O
M58	24.478	567.3508	567.3539	−7.23	6	$C_{30}H_{50}O_7$	dehydrogenated trihydroxylated mogrol	−4Glc − 2H + 3O
M59	25.380	567.3499	567.3539	−5.46	6	$C_{30}H_{50}O_7$	dehydrogenated trihydroxylated mogrol	−4Glc − 2H + 3O
M60	27.050	567.3498	567.3539	−7.05	6	$C_{30}H_{50}O_7$	dehydrogenated trihydroxylated mogrol	−4Glc − 2H + 3O
M61	27.728	567.3520	567.3539	−7.23	6	$C_{30}H_{50}O_7$	dehydrogenated trihydroxylated mogrol	−4Glc − 2H + 3O
M62	24.412	565.3351	565.3382	−5.48	7	$C_{30}H_{48}O_7$	didehydrogenated trihydroxylated mogrol	−4Glc − 4H + 3O
M63	26.052	565.3357	565.3382	−4.42	7	$C_{30}H_{48}O_7$	didehydrogenated trihydroxylated mogrol	−4Glc − 4H + 3O
M64	28.810	565.3368	565.3382	−2.48	7	$C_{30}H_{48}O_7$	didehydrogenated trihydroxylated mogrol	−4Glc − 4H + 3O
M65	30.340	565.3347	565.3382	−6.19	7	$C_{30}H_{48}O_7$	didehydrogenated trihydroxylated mogrol	−4Glc − 4H + 3O
M66	13.872	585.3613	585.3644	−5.30	5	$C_{30}H_{52}O_8$	tetrahydroxylated mogrol	−4Glc + 4O
M67	14.242	585.3601	585.3644	−7.35	5	$C_{30}H_{52}O_8$	tetrahydroxylated mogrol	−4Glc + 4O
M68	14.603	585.3608	585.3644	−6.15	5	$C_{30}H_{52}O_8$	tetrahydroxylated mogrol	−4Glc + 4O
M69	18.307	585.3603	585.3644	−4.95	5	$C_{30}H_{52}O_8$	tetrahydroxylated mogrol	−4Glc + 4O
M70	19.408	585.3613	585.3644	−5.30	5	$C_{30}H_{52}O_8$	tetrahydroxylated mogrol	−4Glc + 4O
M71	15.573	583.3444	583.3488	−7.54	6	$C_{30}H_{50}O_8$	dehydrogenated tetrahydroxylated mogrol	−4Glc − 2H + 4O
M72	15.997	583.3454	583.3488	−8.54	6	$C_{30}H_{50}O_8$	dehydrogenated tetrahydroxylated mogrol	−4Glc − 2H + 4O
M73	20.492	583.3454	583.3488	−6.00	6	$C_{30}H_{50}O_8$	dehydrogenated tetrahydroxylated mogrol	−4Glc − 2H + 4O

Table 1. *Cont.*

No.	t_R (min)	Meas. (Da)	Pred.(Da)	Err. (ppm)	DBE [2]	Formula	Identification	Reactions
M74	20.800	583.3465	583.3488	−3.94	6	$C_{30}H_{50}O_8$	dehydrogenated tetrahydroxylated mogrol	−4Glc − 2H + 4O
M75	21.453	583.3465	583.3488	−3.94	6	$C_{30}H_{50}O_8$	dehydrogenated tetrahydroxylated mogrol	−4Glc − 2H + 4O
M76	22.895	583.3452	583.3488	−6.17	6	$C_{30}H_{50}O_8$	dehydrogenated tetrahydroxylated mogrol	−4Glc − 2H + 4O
M77	24.710	583.3447	583.3488	−7.03	6	$C_{30}H_{50}O_8$	dehydrogenated tetrahydroxylated mogrol	−4Glc − 2H + 4O
M78	20.615	581.3297	581.3331	−5.85	7	$C_{30}H_{48}O_8$	didehydrogenated tetrahydroxylated mogrol	−4Glc − 4H + 4O
M79	21.815	581.3290	581.3331	−7.05	7	$C_{30}H_{48}O_8$	didehydrogenated tetrahydroxylated mogrol	−4Glc − 4H + 4O
M80	23.007	581.3292	581.3331	−6.71	7	$C_{30}H_{48}O_8$	didehydrogenated tetrahydroxylated mogrol	−4Glc − 4H + 4O
M81	23.433	581.3306	581.3331	−4.03	7	$C_{30}H_{48}O_8$	didehydrogenated tetrahydroxylated mogrol	−4Glc − 4H + 4O
M82	23.988	581.3308	581.3331	−3.96	7	$C_{30}H_{48}O_8$	didehydrogenated tetrahydroxylated mogrol	−4Glc − 4H + 4O
M83	25.682	581.3304	581.3331	−4.64	7	$C_{30}H_{48}O_8$	didehydrogenated tetrahydroxylated mogrol	−4Glc − 4H + 4O
M84	25.990	581.3291	581.3331	−4.00	7	$C_{30}H_{48}O_8$	didehydrogenated tetrahydroxylated mogrol	−4Glc − 4H + 4O
M85	17.707	587.2977	587.2992	−2.55	7	$C_{30}H_{48}O_9$	didehydrogenated pentahydroxylated mogrol	−4Glc − 4H + 5O
M86	18.607	587.2983	587.2992	−1.53	7	$C_{30}H_{48}O_9$	didehydrogenated pentahydroxylated mogrol	−4Glc − 4H + 5O

[1] Confirmed by comparison with reference compounds. [2] DBE, double bond equivalent.

2.2.1. Metabolites Formed by Monoglycosylation (**M1**, **M2**)

M1–M2 showed $[M + HCOOH - H]^-$ at m/z 1285.64, which indicated that their molecular formulae were $C_{60}H_{102}O_{29}$. The formulae had an additional glucosyl ($C_6H_{10}O_5$) than that of siamenoside I ($C_{54}H_{92}O_{24}$). Hence, they were mogroside V isomers.

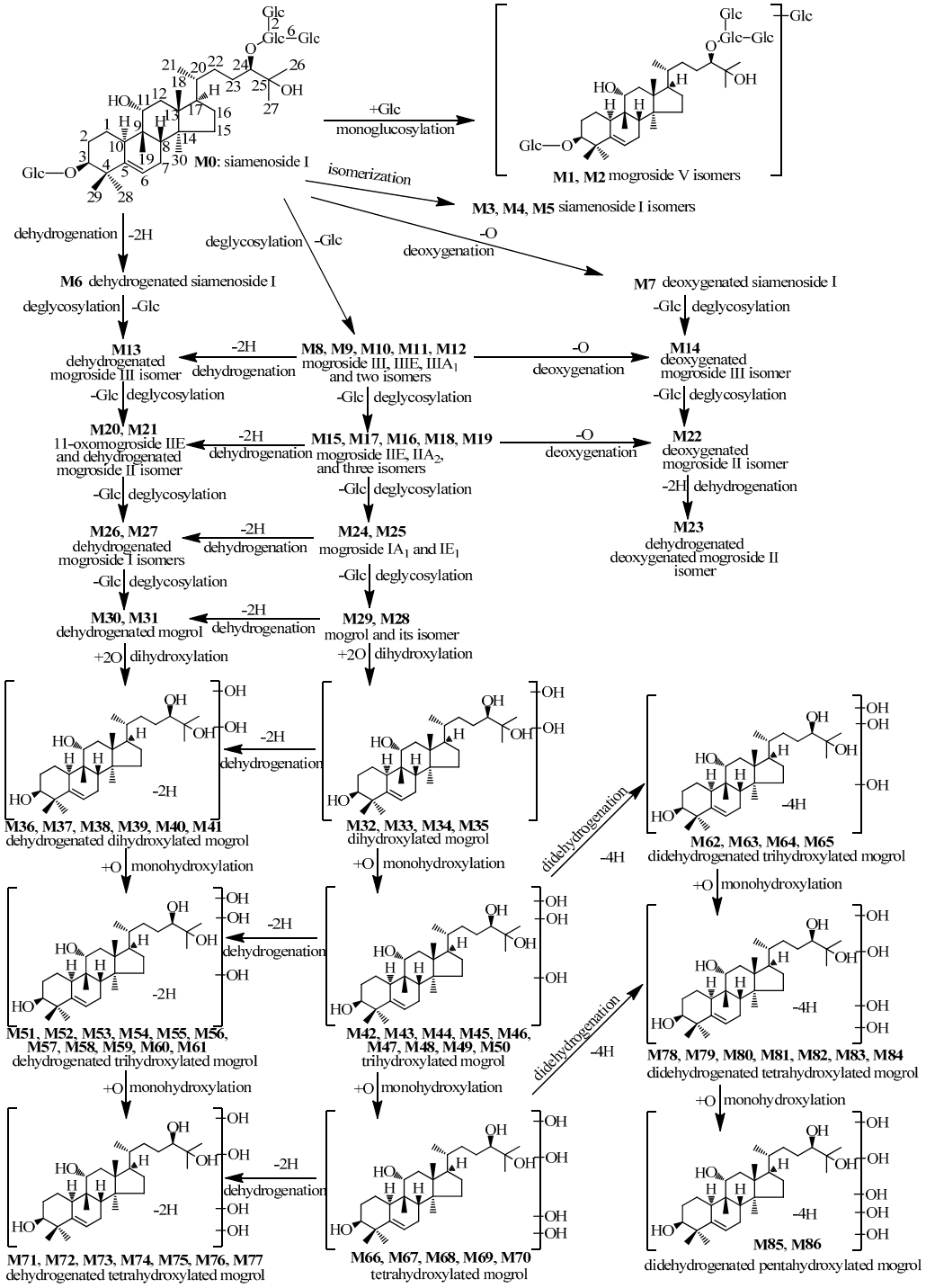

Figure 1. The proposed metabolic pathways of siamenoside I in rats.

2.2.2. Metabolites Formed by Isomerization (**M3**–**M5**)

M3–**M5** showed $[M + HCOOH - H]^-$ at m/z 1169.59, indicating the molecular formula of $C_{54}H_{92}O_{24}$, which was the same to siamenoside I. Hence, they were mogroside IV isomers, and **M3**–**M4** were further confirmed as mogroside IVA and mogroside IVE by comparison with reference compounds.

2.2.3. Metabolites Formed by Dehydrogenation (**M6**)

The molecular formula of **M6** was predicted to be $C_{54}H_{90}O_{24}$ based on its $[M + HCOOH - H]^-$ at m/z 1167.5730, which was formed by loss of two hydrogen atoms from siamenoside I, thus **M6** was tentatively identified as dehydrogenated siamenoside I.

2.2.4. Metabolites Formed by Deoxygenation (**M7**)

The molecular formula of **M7** was $C_{54}H_{92}O_{23}$ calculated from its $[M + HCOOH - H]^-$ at m/z 1153.5957, which has one less oxygen atom than that of siamenoside I. Accordingly, it was tentatively identified as deoxygenated siamenoside I.

2.2.5. Metabolites Formed by Deglucosylation (**M8**–**M12**)

M8–**M12** showed $[M + HCOOH - H]^-$ at m/z 1007.54, implying their molecular formulae of $C_{48}H_{82}O_{19}$. The formulae had one less glucosyl group (element composition: $C_6H_{10}O_5$) than that of siamenoside I, so they were mogroside III isomers. In addition, **M8**–**M10** were unambiguously identified as mogroside III, mogroside IIIE, and mogroside $IIIA_1$ by comparison with reference compounds.

2.2.6. Metabolites Formed by Deglucosylation and Dehydrogenation (**M13**)

M13 had the molecular formula of $C_{48}H_{80}O_{19}$ predicted by its $[M + HCOOH - H]^-$ at m/z 1005.5269. Compared with $C_{48}H_{82}O_{19}$ of mogroside III isomers, it was tentatively identified as dehydrogenated mogroside III isomer. Moreover, in the MS^2 of **M13**, $[M - H - 2Glc]^-$ at m/z 797.4629 ($C_{42}H_{69}O_{14}$), $[M - H - 3Glc]^-$ at m/z 635.4090 ($C_{36}H_{59}O_9$), $[aglycon - H]^-$ at m/z 473.3623 ($C_{30}H_{49}O_4$) were observed. Hence, **M13** was a triglucoside of dehydrogenated mogrol.

2.2.7. Metabolites Formed by Deglucosylation and Deoxygenation (**M14**)

The molecular formula of **M14** was calculated to be $C_{48}H_{82}O_{18}$ by its $[M + HCOOH - H]^-$ at m/z 991.5441, which had one less oxygen atom than $C_{48}H_{82}O_{19}$ of mogroside III, so it was tentatively identified as deoxygenated mogroside III isomer.

2.2.8. Metabolites Formed By Dideglucosylation (**M15**–**M19**)

The molecular formulae of **M15**–**M19** were determined to be $C_{42}H_{72}O_{14}$ based on their $[M + HCOOH - H]^-$ at m/z 845.49, which had one less glucosyl group (element composition: $C_6H_{10}O_5$) than $C_{48}H_{82}O_{19}$ of mogroside III, so they were mogroside II isomers. Furthermore, **M15** and **M17** were confirmed to be mogroside IIE and mogroside IIA_2 by comparison with reference compounds.

2.2.9. Metabolites Formed by Dideglucosylation and Dehydrogenation (**M20**–**M21**)

M20–**M21** showed $[M + HCOOH - H]^-$ at m/z 843.47 in MS, suggesting their molecular formulae of $C_{42}H_{70}O_{14}$. Additionally, they showed $[aglycon - H]^-$ at m/z 473.3623 ($C_{30}H_{49}O_4$) in MS^2 spectra. Therefore, they were tentatively identified as dehydrogenated mogroside II isomer, *i.e.*, diglucoside of dehydrogenated mogrol. Further, **M20** was unambiguously identified as 11-oxomogroside IIE by comparison with reference compounds.

2.2.10. Metabolites Formed by Dideglucosylation and Deoxygenation (**M22**)

M22 was tentatively identified as deoxygenated mogroside II isomer, since its molecular formula was determined to be $C_{42}H_{72}O_{13}$ by its $[M + HCOOH - H]^-$ at m/z 829.4946, which had one less oxygen atom than $C_{42}H_{72}O_{14}$ of mogroside II isomers. In addition, **M22** showed $[M - H]^-$ at m/z 783.4833 ($C_{42}H_{71}O_{13}$), $[M-H-C_6H_{10}O_4$ (deoxyhexosyl)$]^-$ at m/z 637.4252 ($C_{36}H_{61}O_9$), and $[M-H-C_6H_{10}O_4-Glc]^-$ at m/z 475.3742 ($C_{30}H_{51}O_4$) in MS^2 spectra, which indicated that the deoxygenation occurred in hexose and the aglycone was mogrol. Thus, **M22** was identified as a deoxyhexosyl-glucosyl mogrol.

2.2.11. Metabolites Formed by Dideglucosylation, Dehydrogenation, and Deoxygenation (**M23**)

The molecular formula of **M23** was determined to be $C_{42}H_{70}O_{13}$ according to its $[M + HCOOH - H]^-$ at m/z 827.4780, which lost two hydrogen atoms from $C_{42}H_{72}O_{13}$ of **M22**. Consequently, **M23** was tentatively identified as a dehydrogenated deoxygenated mogroside II isomer.

2.2.12. Metabolites Formed by Trideglucosylation (**M24**–**M25**)

M24–**M25** showed $[M + HCOOH - H]^-$ at m/z 683.43 in MS, and $[M-H]^-$ at m/z 637.42 ($C_{36}H_{61}O_9$), [aglycone$-H]^-$ at m/z 475.37 ($C_{30}H_{51}O_4$) in MS^2 spectra, which implied that they were mogrol glucoside. By comparison with the LC-MS^n data in literature [10], **M24** and **M25** were tentatively identified as mogroside IA_1 and mogroside IE_1, respectively.

2.2.13. Metabolites Formed by Trideglucosylation and Dehydrogenation (**M26**–**M27**)

The molecular formulae of **M26**–**M27** were predicted to be $C_{36}H_{60}O_9$ based on its $[M + HCOOH - H]^-$ at m/z 681.42 in MS, which had two less hydrogen atoms than $C_{36}H_{62}O_9$ of mogroside I isomers. In their negative ion (NI) MS^2 spectra, $[M - H]^-$ at m/z 635.41 ($C_{36}H_{59}O_9$) and [aglycone$-H]^-$ at m/z 473.36 ($C_{30}H_{49}O_4$) were detected. As a result, **M26**–**M27** were tentatively identified as glucosides of dehydrogenated mogrol, *i.e.*, dehydrogenated mogroside I isomers.

2.2.14. Metabolites Formed by Tetradeglucosylation (**M28**–**M29**)

M29 was unambiguously identified as mogrol by comparison with reference compound. **M28** had the same molecular formula to mogrol, which showed $[M + HCOOH - H]^-$ at m/z 521.38 in MS, so it was a mogrol isomer.

2.2.15. Metabolites Formed by Tetradeglucosylation and Dehydrogenation (**M30**–**M31**)

M30 and **M31** had the molecular formulae of $C_{30}H_{50}O_4$ predicted by their $[M + HCOOH - H]^-$ at m/z 519.36, which had two less hydrogen atoms than $C_{30}H_{52}O_4$ of mogrol, thus they were tentatively identified as dehydrogenated mogrols.

2.2.16. Metabolites Formed by Tetradeglucosylation and Dihydroxylation (**M32**–**M35**)

M32–**M35** showed $[M + HCOOH - H]^-$ at m/z 553.37, indicating the molecular formula of $C_{30}H_{52}O_6$. Compared to $C_{30}H_{52}O_4$ of mogrol, it had two more oxygen atoms. Accordingly, **M32**–**M35** were tentatively identified as dihydroxylated mogrols.

In addition, the possible hydroxylation sites of **M32** can be deduced by its MS^2 data and one possible structure of **M32** is shown in Figure 2a. The nomenclature for the fragmentation pathways and fragment ions of cucurbitanes proposed by the authors [10] were used in this study.

In MS^2 spectra of **M32**, m/z 433.3011 ($[^{c,j}ABCDE - H]^-$, $C_{27}H_{45}O_4$) generated by $^{c,j}A$ cleavage and m/z 349.2406 ($[^{s,t}DE - H]^-$, $C_{21}H_{33}O_4$) generated by $^{s,t}D$ cleavage were observed, which indicated that one hydroxylation site was in $^{c,j}A$, and the other was in $^{c,j}ABC^{s,t}D$ (Figure 2a).

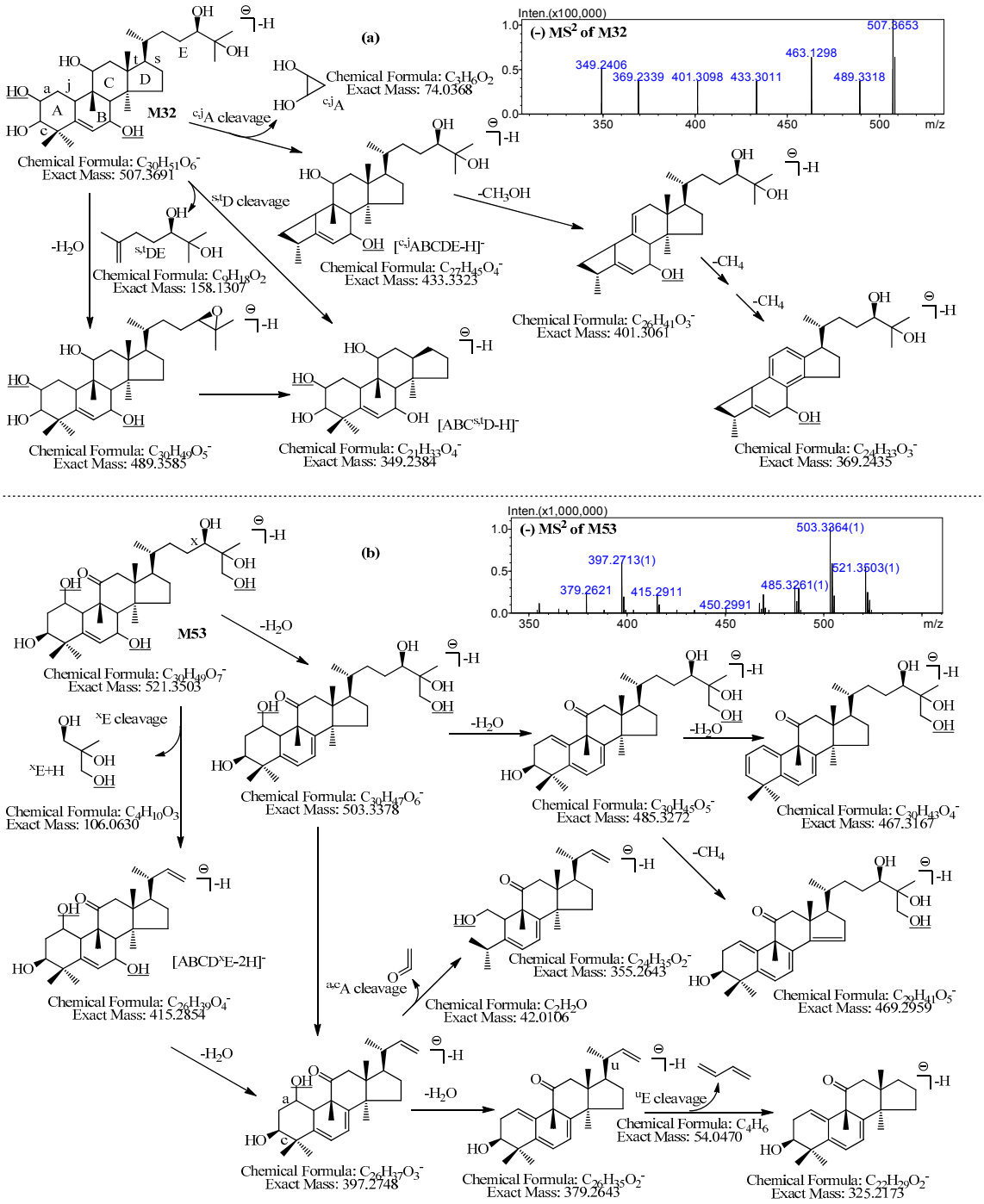

Figure 2. The MS^2 spectra, characteristic fragment ions, and proposed fragmentation pathways of **M32** and **M53**. (**a**) **M32**; (**b**) **M53**.

2.2.17. Metabolites Formed by Tetradeglucosylation, Dihydroxylation, and Dehydrogenation (**M36**–**M41**)

The molecular formulae of **M36**–**M41** were calculated to be $C_{30}H_{50}O_6$ based on their $[M + HCOOH - H]^-$ at m/z 551.35. Compared to $C_{30}H_{52}O_6$ of **M32**–**M35**, it had two less hydrogen atoms. Accordingly, **M36**–**M41** were tentatively identified as dehydrogenated dihydroxylated mogrols.

2.2.18. Metabolites Formed by Tetradeglucosylation and Trihydroxylation (**M42–M50**)

M42–M50 had the molecular formulae of $C_{30}H_{52}O_7$ predicted by their $[M + HCOOH - H]^-$ at m/z 569.36. Compared to $C_{30}H_{52}O_6$ of **M32–M35** (dihydroxylated mogrol), it had one more oxygen atom. Accordingly, **M42–M50** were tentatively identified as trihydroxylated mogrols.

2.2.19. Metabolites Formed by Tetradeglucosylation, Trihydroxylation, and Dehydrogenation (**M51–M61**)

The molecular formulae of **M51–M61** were determined to be $C_{30}H_{50}O_7$ on the basis of their $[M + HCOOH - H]^-$ at m/z 567.35. In comparison with $C_{30}H_{52}O_7$ of **M42–M50** (trihydroxylated mogrol), it had two less hydrogen atoms. As a result, **M51–M61** were tentatively identified as dehydrogenated trihydroxylated mogrols.

Further, the possible hydroxylation sites of **M53** could be deduced by its MS^2 data, and one possible structure of **M53** is shown in Figure 2b.

M53 showed $[M + HCOOH - H]^-$ at m/z 567.3524 in MS, and then it was fragmented into $[M - H]^-$ at m/z 521.3207 ($C_{30}H_{49}O_7$) in MS^2 spectrum. The $[M - H]^-$ was further cleaved into product ions at m/z 503.3364 ($C_{30}H_{47}O_6$), 485.3261 ($C_{30}H_{45}O_5$), and 467.3056 ($C_{30}H_{43}O_4$) formed by sequential losses of H_2O. It was also cleaved into product ion at m/z 415.2911 ($C_{26}H_{39}O_4$) by losing $C_4H_{10}O_3$ (^{x}E+H), which indicated that one hydroxylation site was in ^{x}E. Besides, the characteristic fragment ions at m/z 397.2713 ($C_{26}H_{37}O_3$), m/z 379.2621 ($C_{26}H_{35}O_2$), m/z 355.2613 ($C_{24}H_{35}O_2$), and m/z 325.2449 ($C_{22}H_{29}O_2$) were observed in MS^2, indicating that the other two hydroxylation sites should be located at ^{a,c}ABCD^{u}E (Figure 2b).

2.2.20. Metabolites Formed by Tetradeglucosylation, Trihydroxylation, and Didehydrogenation (**M62–M65**)

M62-M65 had the molecular formulae of $C_{30}H_{48}O_7$ predicted by their $[M + HCOOH - H]^-$ at m/z 565.33, which had two less hydrogen atoms than $C_{30}H_{50}O_7$ of **M51–M61**. Accordingly, **M62–M65** were tentatively identified as didehydrogenated trihydroxylated mogrols.

2.2.21. Metabolites Formed by Tetradeglucosylation and Tetrahydroxylation (**M66–M70**)

M66–M70 showed $[M + HCOOH - H]^-$ at m/z 585.36, indicating the molecular formula of $C_{30}H_{52}O_8$. Compared with $C_{30}H_{52}O_4$ of mogrol, their molecular formula had four more oxygen atoms. Therefore, they were tetrahydroxylated mogrols.

2.2.22. Metabolites Formed by Tetradeglucosylation, Tetrahydroxylation, and Dehydrogenation (**M71–M77**)

The molecular formulae of **M71–M77** were determined to be $C_{30}H_{50}O_8$ based on their $[M + HCOOH - H]^-$ at m/z 583.34, which had two less hydrogen atoms than $C_{30}H_{52}O_8$ of **M66–M70** (tetrahydroxylated mogrol). Accordingly, they were tentatively identified as dehydrogenated tetrahydroxylated mogrol.

Besides, the possible dehydrogenation and hydroxylation sites of **M74** could be deduced by its MS^2 and MS^3 data, and one possible structure of **M74** is shown in Figure 3a.

The characteristic product ions at m/z 479.2977 ($C_{27}H_{43}O_7$, ABCD^{y}E$^-$) produced by ^{y}E cleavage, m/z 419.2762 ($C_{25}H_{39}O_5$) generated by ^{a,c}A cleavage, and m/z 195.1347 ($C_{12}H_{19}O_2$) generated by ^{n,p}C cleavage indicated that the C_{24}-hydroxyl group of **M74** was dehydrogenated, and one of the four tetrahydroxylation sites was at C_2, one was in ^{n,p}CD^{y}E, and the other two were in AB^{n,p}C (Figure 3a).

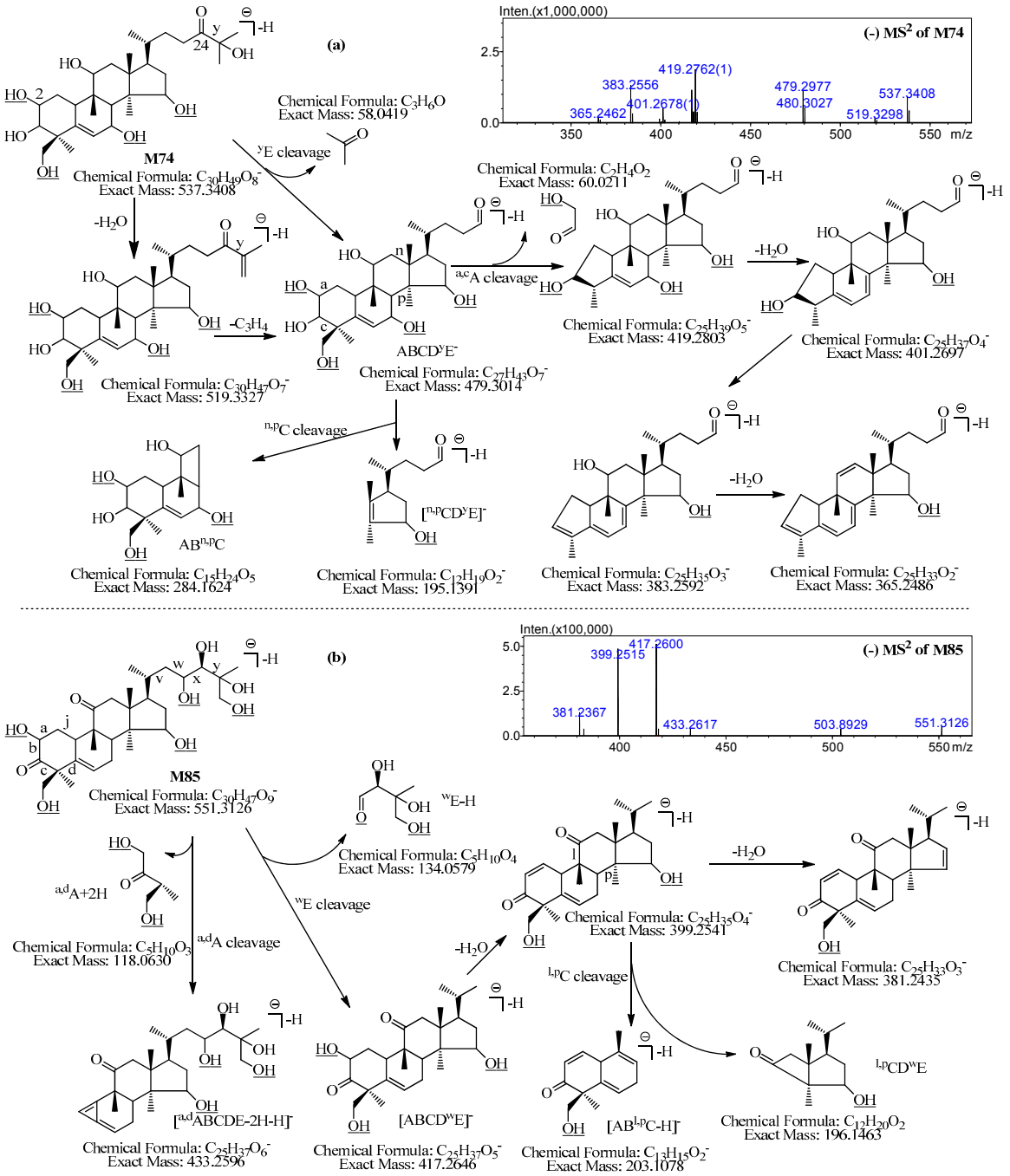

Figure 3. The MS^2 spectra, characteristic fragment ions, and proposed fragmentation pathways of **M74** and **M85**. (**a**) **M74**; (**b**) **M85**.

2.2.23. Metabolites Formed by Tetradeglucosylation, Tetrahydroxylation, and Didehydrogenation (**M78**–**M84**)

M78–**M84** showed $[M + HCOOH - H]^-$ at m/z 581.33 in their MS, indicating their molecular formulae of $C_{30}H_{48}O_8$, which had two less hydrogen atoms than $C_{30}H_{50}O_8$ of **M71**–**M77**. Therefore, **M78**–**M84** were tentatively identified to be didehydrogenated tetrahydroxylated mogrol.

2.2.24. Metabolites Formed by Tetradeglucosylation, Pentahydroxylation, and Didehydrogenation (**M85**–**M86**)

M85–**M86** had the molecular formulae of $C_{30}H_{48}O_9$ predicted by their $[M + HCOOH - H]^-$ at m/z 587.29 in their MS, which had one more oxygen atom than $C_{30}H_{48}O_8$ of **M78**–**M84**. Accordingly, **M85**–**M86** were tentatively identified as didehydrogenated pentahydroxylated mogrol.

In addition, the possible dehydrogenation and hydroxylation sites of **M85** could be deduced by its MS^2 and MS^3 data, and one possible structure of **M85** is shown in Figure 3b.

M85 showed $[M + Cl]^-$ at m/z 587.2977, which was fragmented into $[M - H]^-$ at m/z 551.3126 ($C_{30}H_{47}O_9$) in MS^2 spectrum. The $[M - H]^-$ was then fragmented into characteristic product ions at m/z 433.2617 ($C_{25}H_{37}O_6$, $[^{a,d}ABCDE - 2H - H]^-$) and m/z 417.2600 ($C_{25}H_{37}O_5$, $[ABCD^wE]^-$) by $^{a,d}A$ cleavage and ^wE cleavage respectively, which implied that two of the five hydroxylation sites were in $^{a,d}A$, other two were in ^wE. Furthermore, the ion at m/z 417.2600 ($C_{25}H_{37}O_5$, $[ABCD^wE]^-$) was cleaved into product ions at m/z 399.2515 ($C_{25}H_{35}O_4$) and m/z 203.0987 ($C_{13}H_{15}O_2$) by sequential loss of H_2O and $^{l,p}CD^wE$ ($C_{12}H_{20}O_2$) in MS^3 spectra, which indicated that the last of the five hydroxylation sites was in $^{l,p}CD^wE$.

2.3. Distribution of the Metabolites of Siamenoside I in Rats

The peak areas and distributions of siamenoside I and the 86 identified metabolites in different biological samples are shown in Table 2.

Table 2. Distribution of siamenoside I and its 86 metabolites in rat organs and their peak areas calculated from extracted ion chromatograms (EICs).

No.	Feces	Urine	Plasma	Heart [1]	Liver [1]	Spleen [1]	Lung [1]	Kidney [1]	Stomach [1]	Intestine [1]	Brain [1]	Muscle	TPA [2]
M0	9,489,561	45,194,235	929,711				655,725	1,151,491	15,473,808	1,201,5247	1,162,190		86,071,968
M1	1,144,657	9,555,900							2,001,769	1,487,067	680,786		14,870,179
M2		15,997,951									531,345		16,529,296
M3	760,580	847,869						1,307,673	1,655,097	2,264,310	177,956		7,013,485
M4	545,593	5,114,666			2,993,972	1,200,234		2,991,375	1,454,847	2,022,516	66,665		16,389,868
M5	1,984,320	2,244,041								3,096,436	301,433		7,626,230
M6	1,370,701	24,868,935	522,375				216,179	460,499	5,658,908	2,342,276	8,964,568		44,404,441
M7	151,476	1,610,485											1,761,961
M8	686,710	509,105							9,795,285	3,463,191			14,454,291
M9	5,499,380	4,564,759	247,245	3,396,211	10,439,099	1,349,085	621,654	17,082,221	23,756,273	15,351,670	7,796,211		90,103,808
M10	25,071,251												25,071,251
M11	6,584,321												6,584,321
M12	7,864,503												7,864,503
M13	5,673,582	927,152			1,104,655	1,569,801	126,725	2,884,615	10,255,235		861,731		23,403,496
M14	4,700,498								1,594,595	2,186,093			8,481,186
M15	122,469,048	2,086,502		752,082		1,976,,058			9,533,756	34,065,738			170,883,184
M16	10,029,179												10,029,179
M17	14,873,427								3,964,569				18,837,996
M18	131,377,697	2,775,395				2,221,834		1,382,313	6,051,761		868,285		144,677,285
M19	45,423,120	394,065								8,102,455	562,370		54,482,010
M20	50,669,383					447,658			1,165,195	34,649,284			86,931,520
M21	50,269,416	885,941						128,120	905,385				52,188,862
M22	162,025,962	861,129											162,887,091
M23	29,484,814												29,484,814
M24	180,532,696	352,905						685,128			1,649,227		184,835,243
M25	896,803,169	4,472,844				29,155,815		486,612	21,253,177	297,909,967			1,250,081,584
M26	48,856,108	1,376,742									598,621		50,831,471
M27	790,013,598								2,541,940	18,180,494			810,736,032
M28	92,475,813								1,666,710	1,426,867			95,569,390
M29	646,804,735	459,452						313,543	12,256,309	1,839,703			661,673,742
M30	24,183,728												24,183,728
M31	324,786,331								5,151,046				329,937,377
M32	390,217,566								818,492				391,036,058
M33	46,223,582												46,223,582
M34	125,631,723				2,735,164				1,822,325	1,674,281			131,863,493
M35	488,223,880				1,363,338				8,760,094	4,522,744			502,870,056
M36	33,006,739												33,006,739
M37	23,418,337												23,418,337
M38	46,101,388												46,101,388
M39	27,487,975												27,487,975
M40	20,088,773												20,088,773
M41	27,408,608												27,408,608
M42	12,435,301												12,435,301
M43	77,259,589												77,259,589
M44	284,733,513												284,733,513
M45	44,372,830												44,372,830

Table 2. *Cont.*

No.	Feces	Urine	Plasma	Heart [1]	Liver [1]	Spleen [1]	Lung [1]	Kidney [1]	Stomach [1]	Intestine [1]	Brain [1]	Muscle	TPA [2]
M46	89,188,731												89,188,731
M47	108,520,771												108,520,771
M48	30986,855												30,986,855
M49	34,753,952												34,753,952
M50	53,158,418												53,158,418
M51								15,908,470					15,908,470
M52					30,236,800			43,804,798			2,369,281		76,410,879
M53	463,948,611												463,948,611
M54	21,448,937												21,448,937
M55	79,454,258												79,454,258
M56	79,252,367												79,252,367
M57	39,700,636												39,700,636
M58	86,848,220												86,848,220
M59	17,421,558												17,421,558
M60	21,097,294												21,097,294
M61	88,863,196												88,863,196
M62	38,437,245												38,437,245
M63	102,677,796												102,677,796
M64	35,880,113												35,880,113
M65	23,867,787									1,449,639			25,317,426
M66	13,548,270												13,548,270
M67	5,583,766												5,583,766
M68	5,640,311												5,640,311
M69	9,156,984												9,156,984
M70	10,312,539												10,312,539
M71	13,648,742												13,648,742
M72	4,644,757												4,644,757
M73	54,507,901												54,507,901
M74	77,998,658												77,998,658
M75	39,341,209												39,341,209
M76	12,303,039												12,303,039
M77	7,437,147												7,437,147
M78	30,479,610												30,479,610
M79	45,861,423												45,861,423
M80	18,882,764												18,882,764
M81	285,519,682									1,729,889			287,249,571
M82	19,376,253												19,376,253
M83	36,030,998										26,693,032		62,724,030
M84	14,114,954												14,114,954
M85	30,984,346							27,085,013					58,069,359
M86	50,436,190												50,436,190
TPA [2]	7,540,531,449	125,100,073	1,699,331	4,148,293	50,488,315	37,920,485	1,620,283	115,671,871	147,536,576	449,779,867	53,283,701	0	8,527,780,244
Sum [3]	83	19	2	2	7	7	3	13	21	19	14	0	
Peak Area (A)		$A \geqslant 10^9$	$10^9 > A \geqslant 10^8$		$10^8 > A \geqslant 10^7$		$10^7 > A \geqslant 10^6$		$10^6 > A \geqslant 10^5$		$10^4 \leqslant A < 10^5$		$A = 0$
Color													

[1] These data are comparable. [2] Total peak areas. [3] The total number of metabolites detected.

3. Discussion

The metabolism of siamenoside I in rats was firstly investigated in the present work. In total, 86 new metabolites of siamenoside I were detected in different biological samples from rats, and nine of them were unambiguously identified by comparison with reference compounds, and the others were tentatively identified by careful interpretation of their LC-MS^n data.

3.1. The Metabolic Pathways of Siamenoside I in Rats

Based on the structures of the metabolites (**M1**–**M86**), the metabolic pathways of siamenoside I in rats are proposed and shown in Figure 1. From Figure 1, we can find that the metabolic reactions of siamenoside I include deglycosylation, hydroxylation, dehydrogenation, deoxygenation, isomerization, and glycosylation.

Most of the metabolic reactions of siamenoside I are the same to mogroside V [10]. However, there are also some differences. For example, methylation metabolites were not found in the metabolism of siamenoside I, and deoxygenation is found to be a novel metabolic reaction of mogrosides. Furthermore, pentahydroxylation, didehydrogenation are also found as novel metabolic reactions of mogrosides.

Among 86 metabolites, 63 metabolites (**M6**, **M13**, **M20**, **M21**, **M26**, **M27**, **M30**–**M86**) are formed by oxidation reactions such as hydroxylation and dehydrogenation, and 79 metabolites (**M8**–**M86**) are formed by deglycosylation, which indicate that deglycosylation and oxidation (hydroxylation, dehydrogenation) are the major metabolic reactions of siamenoside I.

Astonishingly, four metabolites (**M7**, **M14**, **M22**, and **M23**) are formed by reduction reaction (deoxygenation). The deoxygenation reaction might occur in hexose, not in aglycone, which is inferred from the identification of **M22** (Section 2.2.10.).

Furthermore, 23 metabolites (**M6**, **M7**, **M13**, **M14**, **M22**, **M23**, **M26**-**M28**, **M30**, **M62**-**M65**, **M78**–**M86**) are firstly reported as new metabolites of mogrosides.

These results suggest that siamenoside I has its own metabolism characteristics in comparison with mogroside V.

3.2. Distribution of the Metabolites of Siamenoside I in Rats

From Table 2, we could find that total peak areas of all detected compounds (siamenoside I and metabolites) in different rat organs are ranked as follows: intestines (449,779,867) > stomach (147,536,576) > kidneys (115,671,871) > brain (53,283,701) > liver (50,488,315) > spleen (37,920,485) > heart (4,148,293) > lungs (1,620,283). In addition, the total numbers of compounds (siamenoside I and metabolites) detected in different organs are in the order of stomach (22) > intestines (20) > brain (15) > kidneys (14) > liver (7) > spleen (7) > lungs (4) > heart (2). Therefore, siamenoside I and its metabolites are mainly distributed to the intestines, stomach, kidneys, and brain.

We also could find the specific metabolites detected in different biosamples. For example, 50 metabolites (**M10**-**M12**, **M16**, **M23**, **M30**, **M33**, **M36**–**M50**, **M53**-**M64**, **M66**–**M80**, **M82**, **M84**, **M86**) are only detected in feces; **M2** is only detected in urine and the brain; **M7** is only detected in urine and feces; **M51** is only detected in kidneys; **M85** is only detected in kidneys and feces; **M17**, **M31**, **M32** are only detected in stomach and feces; **M65** and **M81** are only detected in intestines and feces; **M83** is only detected in brain and feces. Besides, siamenoside I and 14 metabolites (**M1**–**M6**, **M9**, **M13**, **M18**–**M19**, **M24**, **M26**, **M52**, **M83**) are detected in the brain for the first time.

M9 (mogroside IIIE) is detected in all biosamples except muscle, indicating that it is the most widely distributed metabolite.

3.3. The Proposed in Vivo Process of Siamenoside I in Rats

From Table 2, we could find that **M1**–**M29** seem to be the main metabolites, and most of the other metabolites are only detected in feces. We think the reasons for this result may be: (1) the first pass

effect of these metabolites may be very high, *i.e.*, their hepatic extraction ratios are very high, which leads to their very low contents in plasma, organs, and urine samples. As a result, they are not easily detected in these samples; (2) these metabolites are mainly excreted into bile and then to feces, which make their contents in feces high and detectable.

Based on our research results and general metabolic knowledge, we hypothesize that the *in vivo* process of siamenoside I in rats may be as follows.

After oral administration, siamenoside I is degraded into its secondary glycosides (e.g., mogroside III, IIIE, IIIA1, IIE, IIA_2, IA_1, IE_1, *etc.*) and its aglycone (mogrol) or dehydrogenated aglycone (dehydrogenated mogrol) by gastric juice, intestinal juice, intestinal enzymes, or intestinal microflora. Then, mogrol or dehydrogenated mogrol permeate across intestinal mucosa and enter the liver, where they undergo extensive oxidative metabolic reactions to form lots of hydroxylation and/or dehydrogenation metabolites. These polar oxidative metabolites may be largely excreted into the bile and then to the feces, and only a limited amount of them enter general circulation. Besides, some of them may also undergo hepatoenteral circulation and are absorbed into general circulation, and then distributed to different organs, and finally excreted into feces or/and urine.

3.4. Bioactivities of the Metabolites of Siamenoside I

On the basis of literature retrieval, eight metabolites (**M3**, mogroside IVA; **M4**, mogroside IVE; **M8**, mogroside III; **M15**, mogroside IIE; **M24**, mogroside IA_1; **M25**, mogroside IE_1; **M29**, mogrol; **M9**, mogroside IIIE) of siamenoside I can be regarded as bioactive metabolites.

Among them, seven metabolites (**M3**, **M4**, **M8**, **M15**, **M24**, **M25**, **M29**) are able to inhibit the induction of Epstein-Barr virus early antigen by 12-*O*-tetradecanoylphorbol-13-acetate in Raji cells [5]. **M4** and **M9** can inhibit maltase [7]. Hence, they might contribute to the bioactivities of siamenoside I.

4. Materials and Methods

4.1. Chemicals and Reagents

Siamenoside I, mogroside III, mogroside IIIE, mogroside IVE, mogroside V, mogroside IIE, 11-oxomogroside IIE, and mogrol (all purities >98%, determined by HPLC-DAD-ELSD) were isolated from the dried fruits of *Siraitia grosvenorii* and the 50% mogroside V enzymatic hydrolysate by the authors [12,13], and their structures were confirmed by spectral data (UV, IR, NMR and MS). Mogroside IVA, mogroside $IIIA_1$ and mogroside IIA_2 (all purities >98%, determined by HPLC-DAD-ELSD) were purchased from Chengdu MUST Bio-technology Co., Ltd. (Chengdu, Sichuan, China).

Ultra-pure water was prepared by a Millipore Milli-Q Integral 3 Ultrapure Water System (Billerica, MA, USA). Acetonitrile (HPLC grade) was bought from Fisher Chemicals Co. (Fairlawn, NJ, USA) and formic acid (HPLC grade) was purchased from Mreda Technology Inc. (Beijing, China).

4.2. Animals

Sprague-Dawley (SD) rats (male, 210 $\pm$ 20 g) were bought from the Experimental Animal Center of Peking University Health Science Center (Beijing, China). They were handled in agreement with the Guide for the Care and Use of Laboratory Animals of the US National Institutes of Health. All animal experiments were approved by the Biomedical Ethical Committee of Peking University (Approval No. LA2011-058).

4.3. Instruments

A Shimadzu LCMS-IT-TOF instrument was used to perform HPLC-ESI-IT-TOF-MS^n analysis, which consists of a CBM-20A system controller, a DGU-$20A_3$ degasser, two LC-20AD pumps, an SIL-20AC autosampler, a CTO-20A column oven, an SPD-M20A photodiode array (PDA) detector, an ESI ion source, and a hybrid IT-TOF mass spectrometer (Shimadzu, Kyoto, Japan).

4.4. Animal Experiments and Sample Collection

Eight rats were divided into two groups: two were blank group and the others were test group. Each rat was put into a clean metabolic cage (Suzhou Fengshi Laboratory Animal Equipment Co., Suzhou, Jiangsu, China) and given food and water *ad libitum*.

Because the research aim is to find the general/average differences between test group rats (drug-containing sample) and blank group rats (blank sample), the individual differences among the same group rats are not taken into consideration. Accordingly, all of the biosamples from each group were combined into one sample which was more representative than individual samples in the following sample collection processes.

The animal experiment lasted six days. The whole urine and feces of days 1–2 were collected as blank urine and feces samples, respectively. On days 3–5, the rats of test group were orally administrated with siamenoside I [50 mg/kg body weight, in normal saline (NS) solution] at 9:00, and all 72-h urine and feces were collected as drug-containing urine and feces samples, respectively. The rats of blank group were orally administrated with the same volume of NS. On day 6 at 9:00, the test and the blank group were treated with siamenoside I and NS again, respectively. After 1 h, blood sample was collected into a vacuum tube with sodium citrate as anticoagulant (Hebei Xinle Technology Co., Ltd., Shijiazhuang, Hebei, China) from rat heart under anesthesia. Then, the organs (heart, liver, spleen, lung, kidneys, stomach, small intestine, brain) and skeletal muscles of rats were collected and washed with NS, separately. All samples were kept at −80 °C before further pretreatment.

4.5. Sample Preparation

4.5.1. Blood Samples

The blood samples were centrifuged at 3000 rpm for 20 min at 4 °C, and the supernatant plasma samples were collected. Afterward, 8 mL methanol was added to 2 mL of plasma sample, and then was mixed and centrifuged at 9000 rpm for 30 min. The supernatant was collected and evaporated to dryness at 55 °C by a rotatory evaporator. The 15 mg residue was reconstituted in 1.00 mL methanol, filtrated through 0.45 μm filter membrane, and stored at 4 °C before analysis.

4.5.2. Urine Samples

Urine samples were filtered and then evaporated to dryness under vacuum at 55 °C by a rotatory evaporator. Subsequently, the residue was ultrasonically extracted with 10 mL methanol for 30 min, and the extract was then centrifuged at 9000 rpm for 30 min. The supernatant was transferred to another tube and evaporated to dryness at 55 °C by a rotatory evaporator. Next, a 100 mg residue was dissolved in 1.00 mL methanol, filtered through 0.45 μm membranes, and stored at 4 °C before analysis.

4.5.3. Feces Samples

Feces samples were dried at 55 °C and pulverized. Subsequently, the 10 g powder was ultrasonically extracted with 50 mL methanol for 30 min for three times, and the three supernatants were combined and evaporated to dryness. Next, the residue was mixed with 20 mL methanol and centrifuged at 9000 rpm for 30 min. The supernatant was evaporated to dryness again at 55 °C and the residue was collected. Then, 15 mg of residue was dissolved in 1.00 mL methanol, 0.45 μm membranes, and stored at 4 °C before analysis.

4.5.4. Organ and Skeletal Muscle Samples

Each organ was weighed, minced, and homogenized in 4 times volume (mL/g) of 4 °C NS by a homogenizer (Ultra-Turrax T8, Ika-Werke, Gmbh & Co. KG, Staufen, Germany). Then, 10 mL homogenate was mixed with 9 times volume (mL/mL) of acetonitrile, ultrasonically treated for 30 min, and centrifuged at 12,000 rpm for 30 min at 4 °C. Afterward, the supernatant was collected and

evaporated to dryness at 50 °C. The residue was dissolved in 1.00 mL methanol, filtered through 0.45 μm filter membrane, and stored at 4 °C before analysis. The skeletal muscle samples were treated by the same method.

4.6. LC-MS^n Conditions

The column used was Inertsil ODS-3 C_{18} (250 mm × 4.6 mm, 5 μm) (Shimadzu, Kotyo, Japan) protected with a Phenomenex Security Guard column (C_{18}, 4 mm × 3.0 mm, 5.0 μm) (Phenomenex, Torrance, CA). The column temperature was 35 °C. The injection volume of all samples was 20 μL. The mobile phases were water-formic acid (100:0.1, *v*/*v*) (A) and acetonitrile (B).The flow rate was 1.0000 mL/min. A gradient elution program was used: 0.01–10.00 min, 10%–18% B; 10.00–20.00 min, 18%–28% B; 20.00–35.00 min, 28%–45% B; 35.00–60.00 min, 45%–90% B; 60.00–70.00 min, 90%–100% B; 70.00–80.00 min, 100% B. The UV spectrum was recorded from 195 nm to 400 nm.

The parameters of the ESI-IT-TOF-MS^n instrument were: (1) flow rate: 0.2000 mL/min (split from HPLC effluent); (2) positive ion (PI) and negative ion (NI) alternate detection; (3) mass range: MS, *m*/*z* 300–2000; MS^2 and MS^3, *m*/*z* 50–2000; (4) temperature of heat block and curved desolvation line (CDL): 250 °C; (5) nebulizing nitrogen gas flow: 1.5 L/min; interface voltage: (+), 4.5 kV; (−), −3.5 kV; detector voltage: 1.70 kV; (6) ion accumulation time: MS, 30 ms; MS^2 and MS^3, 20 ms; relative collision-induced dissociation (CID) energy: 50%; (7) data-dependent MS^2 and MS^3 fragmentation; (8) All data were recorded and analyzed by LCMS solution Version 3.60, Formula Predictor Version 1.01, and Accurate Mass Calculator (Shimadzu, Kyoto, Japan). The mass range of 50–3000 Da was calibrated by a trifluoroacetic acid sodium solution (2.5 mM).

4.7. Strategy for Profiling and Identification of the Metabolites of Siamenoside I in Biosamples

The strategy [14] previously proposed by the authors was used to find and identify the metabolites of siamenoside I in the present study. In short, the base peak chromatograms (BPCs) of drug-containing samples and blank samples were thoroughly analyzed and compared. Meanwhile, the possible metabolites predicted by general metabolism rules were also screened and confirmed by comparing their corresponding extracted ion chromatograms (EICs). The metabolites were identified by comparison of their retention times and MS^n data with those of reference compounds, or tentatively identified by interpretation of their MS^n data.

4.8. Preliminary Evaluation of the Relative Contents of Siamenoside I and Its Metabolites in Biosamples

To preliminarily estimate the relative contents of siamenoside I and its metabolites in biosamples, the peak area of each metabolite calculated from its NI EIC was used. In the present study, only the data of different organ samples were comparable, since they were prepared and analyzed by the same method.

5. Conclusions

The metabolism of siamenoside I in rats was studied for the first time. In total, 86 new metabolites were detected. Nine of them were unambiguously identified by comparison with reference compounds, and the other 77 were tentatively identified by HPLC-ESI-IT-TOF-MS^n technique. The metabolic pathways of siamenoside I in rats were proposed based on the structures of metabolites. The metabolic reactions of siamenoside I were found to be deglycosylation, hydroxylation, dehydrogenation, deoxygenation, isomerization, and glycosylation, among which deoxygenation, pentahydroxylation, and didehydrogenation were novel metabolic reactions of mogrosides. In addition, 23 metabolites were new metabolites of mogrosides. The distributions of siamenoside I and its 86 metabolites in rat organs were firstly reported, and they were mainly distributed to intestines, the stomach, kidneys, and the brain. Mogroside IIIE was the most widely distributed metabolite. Eight metabolites had bioactivities, indicating that they might contribute to the bioactivities of siamenoside I. These findings not only provide valuable information on the metabolism and disposition of siamenoside I and mogrosides

in rats but also provide useful information on the chemical basis of the pharmacological effects of siamenoside I and mogrosides *in vivo*.

Supplementary Materials: The following are available online at www.mdpi.com/1420-3049/21/2/176, Figures S1–S25: EICs of 86 metabolites in drug-containing sample and blank sample, Table S1: Retention time (t_R), LC-ESI-IT-TOF-MS^n data, molecular formula, and identification of siamenoside I and its metabolites in different biosamples.

Acknowledgments: This study was financially supported by the National Natural Science Foundation of China (No. 81160392) and Guangxi Natural Science Foundation (2014GXNSFBA118049).

Author Contributions: F. Xu and D.-P. Li conceived and designed the experiments; X.-R. Yang, F. Xu, F.-L. Lu, and L. Wang performed the experiments; X.-R. Yang and F. Xu analyzed the data; D.-P. Li, Y.-L. Huang, G.-X. Liu, M.-Y. Shang, and S.-Q. Cai contributed reagents/materials/analysis tools; F. Xu, X.-R. Yang, and D.-P. Li wrote the paper.

Conflicts of Interest: The authors declare no conflict of interest. The founding sponsors had no role in the design of the study; in the collection, analyses, or interpretation of data; in the writing of the manuscript, and in the decision to publish the results.

Abbreviations

The following abbreviations are used in this manuscript:

EBV-EA	Epstein-Barr virus early antigen
TPA	12-*O*-tetradecanoylphorbol-13-acetate
DMBA	9,10-Dimethyl-1,2-benzanthracene
HPLC-ESI-IT-TOF-MS^n	High-performance liquid chromatography-electrospray ionization-ion trap-time of flight-multistage mass spectrometry
Glc	Glucosyl group
NI	Negative ion
DAD-ELSD	Diode array detector coupled with evaporative light scattering detector
NS	Normal saline
BPC	Base peak chromatogram
EIC	Extracted ion chromatogram

References

1. Li, C.; Lin, L.M.; Sui, F.; Wang, Z.M.; Huo, H.R.; Dai, L.; Jiang, T.L. Chemistry and pharmacology of *Siraitia grosvenorii*: A review. *Chin. J. Nat. Med.* **2014**, *12*, 89–102. [CrossRef]
2. Jin, J.K.; Lee, J.H. Phytochemical and pharmacological aspects of *Siraitia grosvenorii*, luo han kuo. *Orient. Pharm. Exp. Med.* **2012**, *12*, 233–239. [CrossRef]
3. Kasai, R.; Nie, R.L.; Nashi, K.; Ohtani, K.; Zhou, J.; Tao, G.D.; Tanaka, O. Sweet cucurbitane glycosides from fruits of *Siraitia siamensis* (chi-zi luo-han-guo), a Chinese folk medicine. *Agric. Biol. Chem.* **1989**, *53*, 3347–3349. [CrossRef]
4. Matsumoto, K.; Kasai, R.; Ohtani, K.; Tanaka, O. Minor cucurbitane glycosides from fruits of *Siraitia grosvenori* (Cucurbitaceae). *Chem. Pharm. Bull.* **1990**, *38*, 2030–2032. [CrossRef]
5. Ukiya, M.; Akihisa, T.; Tokuda, H.; Toriumi, M.; Mukainaka, T.; Banno, N.; Kimura, Y.; Hasegawa, J.; Nishino, H. Inhibitory effects of cucurbitane glycosides and other triterpenoids from the fruit of *Momordica grosvenori* on Epstein-Barr virus early antigen induced by tumor promoter 12-O-tetradecanoylphorbol-13-acetate. *J. Agric. Food Chem.* **2002**, *50*, 6710–6715. [CrossRef] [PubMed]
6. Konoshima, T. Inhibitory effects of sweet glycosides from fruits of *Siraitia grosvenori* on two stage carcinogenesis. *Food Style 21* **2004**, *8*, 77–81.
7. Suzuki, Y.A.; Murata, Y.; Inui, H.; Sugiura, M.; Nakano, Y. Triterpene glycosides of *Siraitia grosvenori* inhibit rat intestinal maltase and suppress the rise in blood glucose level after a single oral Administration of maltose in rats. *J. Agric. Food Chem.* **2005**, *53*, 2941–2946. [CrossRef] [PubMed]

8. Yang, X.W.; Zhang, J.Y.; Xu, W. Biotransformation of mogroside III by human intestinal bacteria. *J. Peking Univ. (Health Sci.)* **2007**, *39*, 657–662.
9. Murata, Y.; Ogawa, T.; Suzuki, Y.A.; Yoshikawa, S.; Inui, H.; Sugiura, M.; Nakano, Y. Digestion and absorption of *Siraitia grosvenori* triterpenoids in the rat. *Biosci. Biotechnol. Biochem.* **2010**, *74*, 673–676. [CrossRef] [PubMed]
10. Xu, F.; Li, D.P.; Huang, Z.C.; Lu, F.L.; Wang, L.; Huang, Y.L.; Wang, R.F.; Liu, G.X.; Shang, M.Y.; Cai, S.Q. Exploring *in vitro*, *in vivo* metabolism of mogroside V and distribution of its metabolites in rats by HPLC-ESI-IT-TOF-MS^n. *J. Pharm. Biomed. Anal.* **2015**, *115*, 418–430. [CrossRef] [PubMed]
11. Liang, J.; Xu, F.; Zhang, Y.Z.; Zang, X.Y.; Wang, D.; Shang, M.Y.; Wang, X.; Chui, D.H.; Cai, S.Q. The profiling and identification of the metabolites of (+)-catechin and study on their distribution in rats by HPLC-DAD-ESI-IT-TOF-MS^n technique. *Biomed. Chromatogr.* **2014**, *28*, 401–411. [CrossRef] [PubMed]
12. Li, D.P.; Ikeda, T.; Nohara, T.; Liu, J.L.; Wen, Y.X.; Sakamoto, T.; Nonaka, G. Cucurbitane glycosides from unripe fruits of *Siraitia grosvenori*. *Chem. Pharm. Bull.* **2007**, *55*, 1082–1086. [CrossRef] [PubMed]
13. Yang, X.R.; Lu, F.L.; Wang, L.; Chen, B.; Xu, F.; Cai, S.Q.; Li, D.P. Methodology of enzymic hydrolysis of fifty percent mogroside V. *Guihaia* **2015**, *35*, 812–816.
14. Liang, J.; Xu, F.; Zhang, Y.Z.; Huang, S.; Zang, X.Y.; Zhao, X.; Zhang, L.; Shang, M.Y.; Yang, D.H.; Wang, X.; *et al*. The profiling and identification of the absorbed constituents and metabolites of Paeoniae Radix Rubra decoction in rat plasma and urine by the HPLC-DAD-ESI-IT-TOF-MS^n technique: A novel strategy for the systematic screening and identification of absorbed constituents and metabolites from traditional Chinese medicines. *J. Pharm. Biomed. Anal.* **2013**, *83*, 108–121. [PubMed]

Sample Availability: Samples of the compounds siamenoside I, mogroside V are available from the authors.